Cognitive Neurodynamics
https://doi.org/10.1007/s11571-023-09991-7

RESEARCH ARTICLE

Motion sickness resistant people showed suppressed steady-state visually evoked potential (SSVEP) under vection-inducing stimulation

Yue Wei[1,2,3] · Yixuan Wang[2,3] · Yuka O. Okazaki[5,6] · Keiichi Kitajo[5,6,7] · Richard H. Y. So[2,3,4]

Received: 10 January 2023 / Revised: 20 June 2023 / Accepted: 2 July 2023

Abstract

Visual stimulation can generate illusory self-motion perception (vection) and cause motion sickness among susceptible people, but the underlying neural mechanism is not fully understood. In this study, SSVEP responses to visual stimuli presented in different parts of the visual field are examined in individuals with different susceptibilities to motion sickness to identify correlates of motion sickness. Alpha band SSVEP data were collected from fifteen university students when they were watching roll-vection-inducing visual stimulation containing: (1) an achromatic checkerboard flickering at 8.6 Hz in the central visual field (CVF) and (2) rotating dots pattern flickering at 12 Hz in the peripheral visual field. Rotating visual stimuli provoked explicit roll-vection perception in all participants. The motion sickness resistant participants showed reduced SSVEP response to CVF checkerboard during vection, while the motion sickness susceptible participants showed increased SSVEP response. The changes of SSVEP in the presence of vection significantly correlated with individual motion sickness susceptibility and rated scores on simulator sickness symptoms. Discussion on how the findings can support the sensory conflict theory is presented. Results offer a new perspective on vection and motion sickness susceptibility.

Keywords Vection · SSVEP · Motion sickness susceptibility

Abbreviations

BC	Background condition
CC	Control condition
RC	Rotation condition
RV	Rotation condition with vection perception
RN	Rotation condition with no-vection

✉ Yue Wei
yweiaj@connect.ust.hk

1 Department of Basic Psychology, School of Psychology, Shenzhen University, 3688 Nanhai Avenue, Nanshan District, Shenzhen 518060, China

2 HKUST-Shenzhen Research Institute, 9 Yuexing First Road, South Area, Hi-Tech Park, Nanshan, Shenzhen 518057, China

3 Bio-Engineering Graduate Program, School of Engineering, The Hong Kong University of Science and Technology, Hong Kong, China

4 Department of Industrial Engineering and Decision Analytics, The Hong Kong University of Science and Technology, Hong Kong, China

5 Division of Neural Dynamics, Department of System Neuroscience, National Institute for Physiological Sciences, National Institutes of Natural Sciences, 38 Nishigonaka, Myodaiji, Okazaki, Aichi 444-8585, Japan

6 Department of Physiological Sciences, School of Life Science, The Graduate University for Advanced Studies (SOKENDAI), 38 Nishigonaka, Myodaiji, Okazaki, Aichi 444-8585, Japan

7 CBS-TOYOTA Collaboration Center, RIKEN Center for Brain Science, Wako, Saitama 351-0198, Japan

Published online: 17 July 2023

CVF	Central visual field
PVF	Peripheral visual field
EEG	Electroencephalographic
EOG	Electrooculogram
EOI	Electrode of interest
FOV	Field of view
MS	Motion sickness
MSSQ	Motion Sickness Susceptibility Questionnaire
MSsus	Motion sickness susceptible
MSres	Motion sickness resistant
VEP	Visual evoked potential
SSVEP	Steady-state Visually Evoked Potential
SSQ	Simulator Sickness Questionnaire

Introduction

When exposed to coherent patterns of visual motion, stationary viewers can experience the illusory sensation of self-motion, which is often termed 'vection' (Palmisano et al. 2015). The utilization of vection is crucial for the user experience and the effectiveness of virtual reality (VR) technologies (Riecke 2011; Riecke et al. 2004). However, for some VR users, vection experience is frequently reported together with motion sickness (MS) (Keshavarz et al. 2015b; Zhang et al. 2015), an unpleasant response with symptoms including gastrointestinal discomfort, oculomotor disturbance and disorientation (Griffin 1990; Kennedy et al. 1993). Currently, the mechanism underlying this phenomenon is not fully understood (Berti and Keshavarz 2020; Keshavarz et al. 2015b; Palmisano et al. 2015). Further explorations on its neurological basis could provide theoretical support for VR users to avoid MS while experiencing vection. Since electroencephalographic (EEG) possesses a good time–frequency resolution, it can enable more elaborate explorations on the dynamic neurological responses during the vection perception. Researchers have been advocating more investigations to be geared by the EEG (Keshavarz et al. 2015a; Palmisano et al. 2015).

Vection and MS susceptibility

With prolonged exposure to vection-inducing stimulation, some susceptible people would experience MS, while others who appear to be resistant to MS, do not (Golding et al. 2012; Miyazaki et al. 2015). The mechanism behind individual susceptibility to the MS provoked by vection-inducing stimulation is not well understood. Based on the most widely recognized 'sensory conflict theory', MS is caused by conflicts between the visual motion perception and vestibular input (Keshavarz et al. 2014; Reason 1978; Zhang et al. 2015). According to the 'reciprocal inhibition hypothesis' (Brandt et al. 1998, 2002), people can suppress the neural activity of visual area or vestibular area to reduce the sensory conflicts. Based on this hypothesis, MSres people should demonstrate a reduction of neurological activities during vection, while MSsus people should not. However, this hypothesis has not been directly examined among people with different MS susceptibility during vection. Most neurological vection studies did not report individual MS susceptibility of participants (Berti et al. 2018; Dowsett et al. 2020; Keshavarz et al. 2015b; Keshavarz and Berti 2014; Kleinschmidt et al. 2002; Thilo et al. 2003; Vilhelmsen et al. 2015). And for most studies focused on MS, researchers usually contrast neurological responses between the control and MS-provoking stimuli, where vection was hardly measured or controlled (Farmer et al. 2015; Miyazaki et al. 2015; Napadow et al. 2013). In those studies, the vection perception may be confounded with the different visual stimulation. Therefore, the current study was designed to fill this gap by directly comparing the EEG correlates of vection perception between MSsus people and MSres people.

Central and peripheral vision

Another crucial confounding factor that may influence the neurological activities during vection, is the visual location occupied by visual stimuli. When viewers are experiencing vection, their central and peripheral vision play different roles (Warren and Kurtz 1992). Moreover, it was found that the behavioural responses to CVF stimuli rather than PVF stimuli were suppressed during vection (Wei et al. 2018). Therefore, to better explore the EEG correlates and MS susceptibility, it is essential to examine the EEG responses correlated to CVF and PVF stimulation, respectively. Although some other EEG based vection studies attempted to present different stimulation to CVF and PVF (Keshavarz and Berti 2014; Stróżak et al. 2016; Thilo et al. 2003), the collected EEG responses were analysed together in their designs. Indeed, most of the previous EEG research on vection studied transient VEPs (Barry et al. 2014; Berti et al. 2018; Berti and Keshavarz 2020; Keshavarz and Berti 2014; Stróżak et al. 2016; Thilo et al. 2003; Vilhelmsen et al. 2015), which reflected the holistic response of a transient trial. Moreover, the meaning of changes in transient visual evoked potential (VEP)

amplitude can be ambiguous, as increase or decrease in different transient VEP components can generate similar difference waves (Luck 2005; Niedermeyer and Lopes da Silva 2005). In this study, we studied steady-state VEP (SSVEP) because different areas of visual field can be tagged with different frequencies in SSVEP (Vialatte et al. 2010). By applying different flickering frequencies to CVF and PVF stimuli, the response to a specific visual location (namely CVF and PVF, respectively) shall be tagged and captured by the SSVEP power at corresponding stimulation frequency (Camfield et al. 2012; Morgan et al. 1996; Müller et al. 1998). Furthermore, the power changes of SSVEP were associated with the activation or suppression of visual processing without ambiguity (Müller et al. 1998; Vialatte et al. 2010).

Hypotheses

In this study, to better explore the neural mechanism behind MS provoked by vection-inducing stimulation, we examined the SSVEP under vection between MSsus people and MSres people, with different frequencies tagged to CVF and PVF stimulation. Based on the 'sensory conflict theory' (Reason 1978) and 'reciprocal inhibition hypothesis' (Brandt et al. 2002), the suppression of neural activity in visual area during vection is associated with less sensory conflict and less MS. Thus, we hypothesize that MSres people should exhibit suppression effects associated with vection as part of their ways to reduce sensory conflict, while MSsus people shall not (**H1a**), with the effect size significantly correlate with individual MS-susceptibility (**H1b**). As previous work suggested that the suppression of visual system is associated with CVF rather than PVF (see Sect. 1.2), we hypothesize that the vection effects reflected by SSVEP power in **H1** shall interact with visual location (**H2**).

Method

To test our hypotheses, this study manipulated and examined combinations of between and within-subject variables (see Table 1). Specifically, we studied the amplitude and topography of SSVEP when different MS susceptibility groups were exposed to a rotation condition (RC) stimulation and a control condition (CC) stimulation presented to their peripheral vision. To generate traceable SSVEP responses, flickering at two different frequencies of alpha bands were added to the RC stimuli (PVF:12 Hz, CVF:8.6 Hz; see Sect. "Visual stimuli"). To investigate the effects of vection, the periods under RC, which reported with vection or without vection by participants, were analysed and compared in each trial (see Sect. "Trial procedure: SSVEP and vection conditions") (Morgan et al. 1996; Müller et al. 1998; Wei et al. 2018).

Participants

Fifteen right-handed university students (24–27 years old, mean 25.40, SD 1.40) were recruited with complete informed consent. Participants filled in the short form of Motion Sickness Susceptibility Questionnaire (MSSQ) before the experiment. Based on previous findings (Wei et al. 2019; Zhao 2017), eight participants who scored higher than the 50th percentile of MSSQ scores (either MSSQ total scale or any subscales) reported in Golding (1998, 2006)'s surveys were assigned to the MS susceptible (MSsus) group and other participants was assigned to the MS resistant (MSres) group. Both groups had a mix of gender (MSsus: 62.5% male; MSres: 71.4% male). There was no significant between-group difference in gender and age (see Table 2 for group summary of demographics, vection and Simulator Sickness Questionnaire [SSQ] reports). All of the participants attained 20/20 visual acuity (Vision Tester: Stereo Optical CO. Inc. U.S.A., Model 2000). All participants were free of any vestibular injury or medical treatment. None of them have rich experience with large-screen visual motion stimuli or video games.

Table 1 Illustration of levels and variables

Between-subject		Within-subject		
MS susceptibility (2 levels)		Visual stimuli (2 levels)	Flicker frequency (2 levels)	Vection perception (2 levels)
MSsus group (N = 8)	MSres group (N = 7)	Rotation condition (RC)	CVF-8.6 Hz and PVF-12 Hz	RN
				RV
		Control condition (CC)	–	–

MSsus Motion sickness susceptible, *MSres* Motion sickness resistant, *CVF* Central visual field, *PVF* Peripheral visual field, *RV* Rotation condition with vection perception, *RN* Rotation condition with no-vection perception

Table 2 Demographics and experiment measures of the MSsus Group and MSres Group

	MSsus group	MSres group	*P*
Age (years)	25.5 ± 1.2	25.3 ± 1.7	0.780
Gender (% male)	62.5%	71.4%	
MSSQ score			
Child (0–27)	9.5 ± 3.1	2.0 ± 1.5	< 0.001***
Adult (0–27)	7.7 ± 3.2	1.1 ± 1.0	< 0.001***
Total (0–54)	17.1 ± 5.1	3.1 ± 2.2	< 0.001***
Pre-SSQ total score (0–40)	0.8 ± 1.7	0.4 ± 0.8	0.570
Post-SSQ total score (0–40)	4.0 ± 5.2	0.4 ± 0.5	0.097^
Post-SSQ_N (0–66.7)	4.8 ± 5.1	0.0 ± 0.0	0.029*
Post-SSQ_O (0–53.1)	8.5 ± 11.0	3.2 ± 4.1	0.24
Post-SSQ_D (0–97.4)	8.7 ± 12.7	0.0 ± 0.0	0.095^
Vection report			
Mean Intensity (1–5)	2.5 ± 0.6	2.3 ± 0.4	0.574
Vection duration (%)	44.0 ± 17.2	46.3 ± 15.8	0.794
Total clean epochs	1275.1 ± 245.4	1228.9 ± 225.0	0.711
RV epochs	435.4 ± 257.5	461.6 ± 257.5	0.821
RN epochs	664.1 ± 246.1	581.6 ± 165.4	0.467
CC epochs	175.6 ± 28.0	185.7 ± 27.6	0.495

***$p < 0.001$, *$p < 0.05$, ^$p < 0.1$. Post-SSQ_O, Post-SSQ_D, Post-SSQ_N represent the score of the ocular motor symptom subscale, the disorientation symptom subscale and the nausea symptom subscale respectively. Except the MSSQ scores and Post-SSQ_N, none of the group comparisons are significant; Note that the SSQ score of the MSsus group was significantly higher than MSres after the experiment on the nausea scale ($p = 0.029$), but the severity of overall sickness remained very low (4 in 40)

Visual stimuli

Since previous studies suggested that the amplitude of alpha band SSVEPs was closely connected to visual suppression (Klimesch 2012; Morgan et al. 1996; Vialatte et al. 2010) and vection (Dowsett et al. 2020), in the current study, the visual stimulation was designed to flip at alpha band frequencies. To elicit roll vection, the rotating dots pattern used in past studies was presented at PVF (Wei et al. 2018, 2019), while a checkerboard similar to the one used in previous studies (Thilo et al. 2003; Wei et al. 2017b) was presented at CVF (Fig. 1a). The stimuli were shown on a 46-inch LCD monitor (screen size: 102.1 × 57.5 cm; field of view: 93.5° × 61.8°; viewing distance: 48 cm) with 650–750 dots visible under all conditions. The achromatic checkerboard occupied a field of view (FOV) of 11.4° × 15.1°. To evoke SSVEP, the rotating dots in the PVF alternated between strong contrast (91.62%; dot luminance: 1.6 cd/m^2) and weak contrast (26.32%; dots luminance: 0.12 cd/m^2) at a frequency of 12 Hz, while the contrast of the checkerboard in CVF was reversed at a frequency of 8.6 Hz (luminance: 10 cd/m^2 for white cells; 0.62 cd/m^2 for black cells; contrast: 88.32%). The selection of these two alpha band frequencies (8.6 Hz and 12 Hz) was based on previous SSVEP studies (Morgan et al. 1996) to ensure the separability and feasibility of the collected SSVEPs. Moreover, we conducted a pilot study to ensure that the flickering stimulation does not damage the vection perception of participants. In RC, all grey dots rotated anticlockwise coherently with an angular velocity of 32°/s. In CC, no flickering was applied in both CVF and PVF, and the grey dots moved in random directions with similar speeds as the dots in RC. Similar CC was used in previous experiments (Brandt et al. 1998; Wei et al. 2018, 2019).

Procedures

Trial procedure: SSVEP and vection conditions

As illustrated in Fig. 1, each trial started with a 1.5 s-baseline black background condition (BC), followed by a 15 s presentation of RC. During the RC, participants were instructed to press a key with their right hand to indicate the onset or cessation of roll vection perception. Therefore, each RC would be divided into sections labeled as with or without vection according to the subject's key pressing. All participants watched one trial of demo stimuli demonstration and received training on how to recognize the state of self-rotational vection. Within each trial, recorded SSVEP in RC when participants were experiencing vection (RV) or experiencing no vection (RN) were compared. Similar to

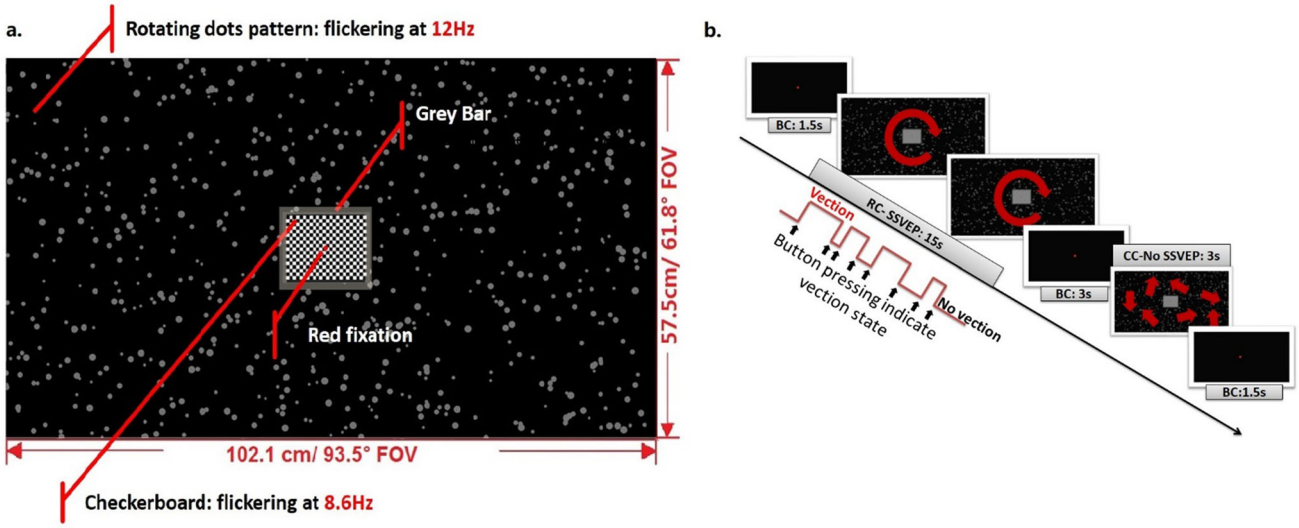

Fig. 1 Stimuli and composition of a trial. *Note*: **a** A snap shot of the stimulus during rotation condition (RC) and **b** a time-line illustration of a single trial consisting sequences of background condition (BC); RC and control condition (CC). The averaged luminance for black cells in checkerboard is 0.62 cd/m^2, and that for white cells is 10 cd/m^2, so the contrast is 88.32%; Note that checkerboard is encircled by grey bar with a luminance of 1.54 cd/m^2 and a width of 0.53 cm; the highlighted grey area is just for illustration, so it is larger than actual stimuli; checkboard has 24 × 18 cells with a size of 0.53 cm. The achromatic checkerboard occupied 11.4 × 15.1°of the field of view (FOV)

previous works (Kleinschmidt et al. 2002; Wei et al. 2019), SSVEPs recorded within 2 s of the perception state change (from vection to no-vection, or vice versa) were excluded as they were still in transition period. Following the 15 s-RC was a 3 s-BC. Then CC stimulation was presented for 3 s. Finally, after CC, each trial ended with a 1.5 s-BC (see Fig. 1b). The total duration of each trial was 24 s (1.5 s + 15 s + 3 s + 3 s + 1.5 s = 24 s). To avoid the confounding effects introduced by visual fatigue and nausea symptoms, the length of trial cannot be too long. It was set as 15 s because pilot data and previous findings suggest that 15 s was enough to provoke vection (Wei et al. 2019). During each trial, participants were instructed to fixate their eyes on a central red dot (diameter: 0.6° of FOV; luminance: 5.05 cd/m^2) to suppress optokinetic nystagmus and other types of eye movements. This served as a control to reduce influence of eye movements on MS (Yang et al. 2011). A chinrest was used to limit head and body movement and fixed the view distance at 48 cm for all participants. To eliminate visual distractions, all lights were switched off. Both the TV and participants were covered with a large black curtain.

Block procedure: attention modulation conditions

Each block consisted of 8 repeated trials (24 s × 8 = 192 s per block). During the experiment, participants followed instructions to carry out three types of attention allocation task: (1) central focus (CF: participants were instructed to concentrate on the central checkerboard and ignore the peripheral rotating stimuli); (2) peripheral focus (PF: participants were instructed to focus on the peripheral rotating stimuli and ignore the central checkerboard stimuli); and (3) no focus requirement (NF: participants were instructed to give attention to the whole screen without any particular focus). In each block, the same task would be presented in all eight repeated trials. All participants completed six repeated NF blocks and six repeated attention focused blocks with three blocks for CF and three for PF. The order of presenting the blocks was randomized. Between successive blocks, participants rested for 3–10 min, until they reported no fatigue or discomfort. In this study, only six NF blocks were analyzed and reported to be focused on the topic. The results of the other blocks would report in other documents.

All stimuli and the EEG synchronization triggers were programmed in MATLAB using Psychtoolbox-3 extensions (Brainard 1997; Pelli 1997). The experiment took place inside an acoustic booth with all parts of the set-up the same as previous research (Wei et al. 2019). The booth reduced electrical interference. All procedures were approved by the human subject and ethics committee of the Hong Kong University of Science and Technology.

Response measures

Measurements of EEG signals

During stimuli presentation, the 32-channel EEG signals were recorded together with two horizontal

Electrooculogram (EOG) (left and right) channels and two vertical EOG (upper and lower) channels using a NuAmps Amplifier (DC-coupled, 22 bits, monopolar) from Ag/AgCl sintered electrodes (Quik-Cap, Compumedics Neuroscan) based on the international 10–10 system referenced to the average of left and right mastoid signals. Impedances between all channels and ground channel (AFz) were kept below 5 kΩ.

Raw EEG data were digitized at a sampling rate of 1000 Hz and a bandwidth of DC-260 Hz, and then filtered offline with an FIR band-pass filter from 1.6 to 45 Hz. The refreshing rate of the monitor was 60 Hz supporting the flipping of dots at PVF at every fifth frame (12 Hz), and the flipping of the checkerboard at CVF at every seventh frame (8.6 Hz). One complete cycle of visual flicker was defined as $5 \times 7 = 35$ frames. Duration of each frame was 16.7 ms and the total duration of one complete cycle was 583 ms. EEG data were segmented into epochs of 1167 ms duration covering the duration of two consecutive complete cycles of the visual flickers. During the period of one epoch, participants were exposed to 10 cycles of 8.6 Hz flickering at CVF and 14 cycles of 12 Hz flickering at PVF. Consecutive epochs were 50% overlapped. Incomplete epochs and epochs covering the transition period (onset or cessation of vection) were discarded. Independent components analysis (ICA) was applied using EEGLAB (Delorme and Makeig 2004), and components identified as eye movement artifacts were removed using an automatic toolbox ADJUST (Mognon et al. 2011). The epochs contaminated by other artifacts were rejected based on a moving window peak-to-peak method (window size: 200 ms; step: 50 ms; threshold: ± 100 μV) and extreme value of remaining ICA components (threshold: ± 20 μV). Current source density analysis was also applied to exclude the potential influence of volume conduction (parameters: the order of spline, m = 4; precision of 1.0e−5) at each electrode position (Kayser and Tenke 2006a, b). The average numbers of valid epochs per participant per analysis condition remained for each condition are listed in Table 2 with standard deviations. In summary, two types of condition contrasts were analyzed: CC (control condition) versus RC (rotation condition); RV (rotation condition with vection) versus RN (rotation condition without vection).

SSVEP analysis

The valid epochs per participant were averaged within each analysis condition and transformed into a power spectrum using ERPLAB Toolbox for SSVEP analysis (Lopez-Calderon and Luck 2014). The 1167 sample epoch (1167 ms sampled at 1000 Hz) was zero pad to 2048 samples before FFT transformation with Hamming window and frequency resolution of 0.2441 Hz. Energy points closest to 12 Hz (PVF stimuli) and 8.6 Hz (CVF stimuli) were extracted as SSVEP power using Fieldtrip (Oostenveld et al. 2011) and EEGLAB (Delorme and Makeig 2004). Topographies of the SSVEP power differences between RC (RV + RN) and CC at the frequencies of CVF and PVF stimulation were analyzed to identify the electrodes of interest (EOIs, Fig. 2).

Reports of vection and SSQ

Participants were trained to report their vection intensity after each block, based on a 5-point scale revised from previous studies (1 = no vection; 5 = saturated vection; Webb and Griffin 2003; see Appendix I.1). The percentage of vection duration under each condition was calculated from the response of participants. To monitor the MS symptoms, all participants completed the Simulator Sickness Questionnaire (SSQ) before and after experiment (Kennedy et al. 1993).

Results

SSVEP power topography

The average power spectra of the SSVEP responses to rotating dot condition (RC) are shown in Fig. 2. As expected, spectral energies of SSVEPs peaked around 8.6 Hz (CVF stimuli frequency) and 12 Hz (PVF stimuli frequency) with their respective harmonics.

To determine the spatial distribution of the SSVEP power at stimuli frequencies, the topography of the RC at 8.6 Hz and 12 Hz were averaged for each group. As showed in Fig. 2, the strongest response to PVF stimulation (12 Hz) was located around the Pz electrode in both groups. As for the response to CVF stimulation (8.6 Hz), the strongest response was located around the Oz electrode for the MSres group, while for the MSsus group, it was located around the P4 electrode. Based on the topography, we selected the EOIs for further analysis: for 12 Hz the Pz electrode was selected as the EOI for all participants; for 8.6 Hz, as MSsus and MSres participants demonstrated two different EOIs (see Fig. 2a), the electrode with stronger power between P4 and Oz were selected as the EOI for each participant (see Fig. 2b). To test whether the SSVEP power of EOIs at RC were significantly different from noise (the control condition: CC), two-way repeated-measures MANOVA was conducted with two within-subject factors (SSVEP stimuli: RC/CC; stimuli frequency: 8.6/12 Hz). The main effect of SSVEP stimuli was significant, showing the SSVEP power of RC was significantly higher than CC [$F(1,14) = 27.019$, $p < 0.001$, Cohen's $f = 1.275$]. The simple-main effect of SSVEP stimuli for 8.6 Hz

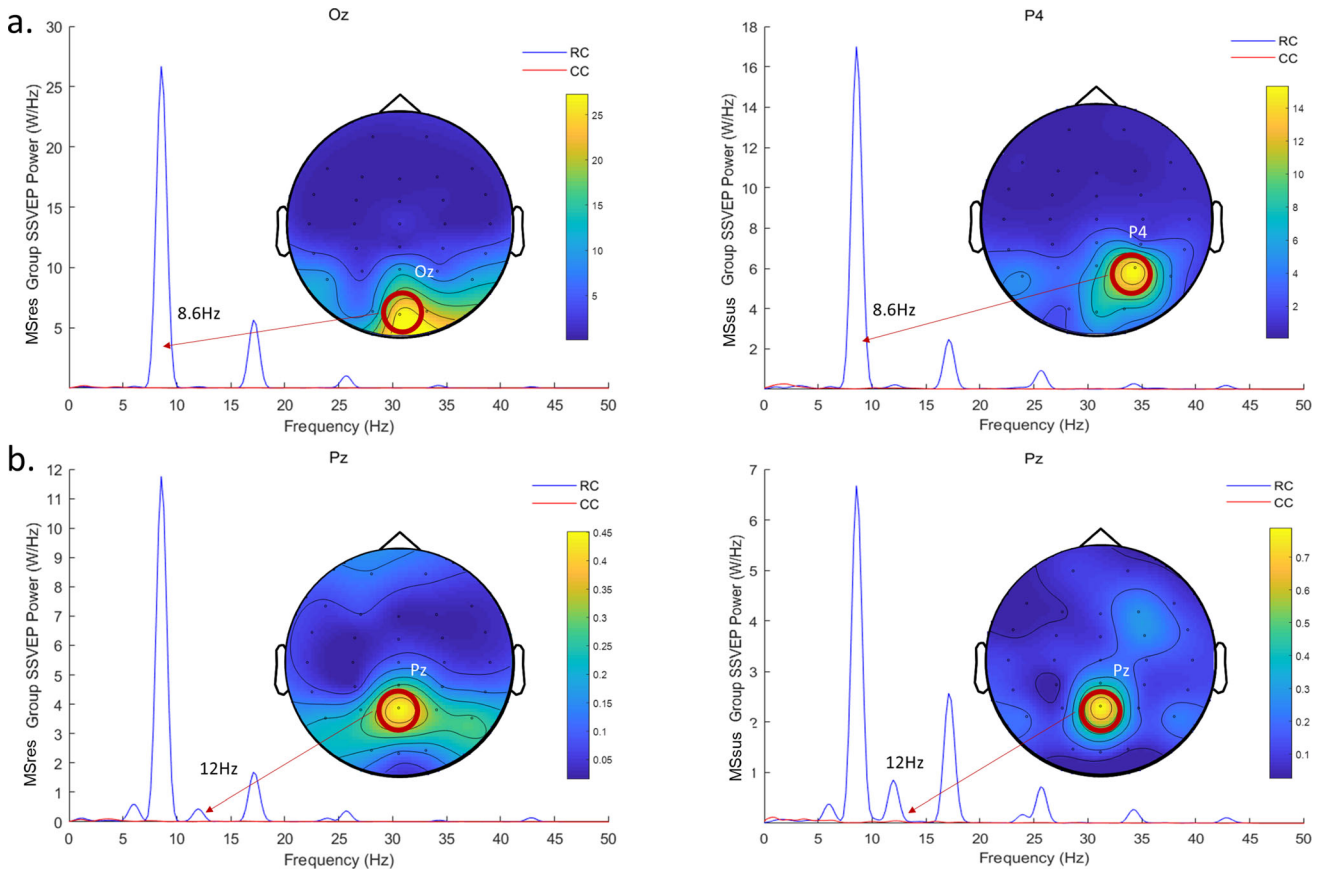

Fig. 2 The power spectrum and topography of SSVEP power at Rotation condition (RC). *Note*: **a** The topography of SSVEP power at CVF stimulus frequency (8.6 Hz) and the power spectrum of EOIs: Oz for MSres Group (left) and P4 for MSsus Group (right). **b** The topography of SSVEP power at PVF stimulus frequency (12 Hz) and the power spectrums at Pz for two groups: MSres Group (left) and MSsus Group (right)

[$F(1,14) = 25.902$, $p < 0.001$, Cohen's $f = 1.248$] and 12 Hz [$F(1,14) = 7.436$, $p = 0.016$, Cohen's $f = 0.634$] were also both significant, showing the SSVEP power of RC was significantly higher than CC for both of the two frequencies.

Vection state effects

We obtained the neural responses indicated by SSVEP power at each stimulus frequency from EOIs selected above. A three-way mixed-measures ANCOVA was conducted with two within-subject factors (vection: RV/RN; stimuli frequency: 8.6/12 Hz) and one between-subject factor (MS susceptibility: MSsus/MSres). The general SSVEP power of RC condition at 8.6 Hz and 12 Hz were added as correlates in the model.

The main effect of MS susceptibility is marginally significant, with MSsus group demonstrating stronger responses than MSE group [$F(1,11) = 4.525$, $p = 0.057$, Cohen's $f = 0.521$]. The interaction of vection × MS susceptibility was significant [$F(1,11) = 11.787$, $p = 0.006$, Cohen's $f = 0.911$]. The interaction of frequency × MS susceptibility was also significant [$F(1,11) = 5.618$, $p = 0.037$, Cohen's $f = 0.596$]. In particular, the interaction of vection × frequency × MS susceptibility was significant [$F(1,11) = 11.886$, $p = 0.005$, Cohen's $f = 0.915$], which supported the **H2** (the vection effect interacts with visual location).

To illustrate the interaction of vection effects, we tested simple-effects under 8.6 Hz (CVF stimuli frequency) and 12 Hz (PVF stimuli frequency) respectively. For 8.6 Hz, the simple-main effect of MS susceptibility was significant, with MSsus group showing stronger responses than MSres group [$F(1,11) = 5.055$, $p = 0.046$, Cohen's $f = 0.559$]. The simple-main effect of vection was not significant. The simple-interaction of vection × MS group was significant [$F(1,11) = 11.911$, $p = 0.005$, Cohen's $f = 0.916$], with MSsus group showing stronger suppression effect under vection (see Fig. 3a for illustration) in supporting of the **H1a**. To further explore the interaction of vection effect × MS susceptibility, we conducted two-tailed paired-sample *t*-tests between RN and RV condition for the

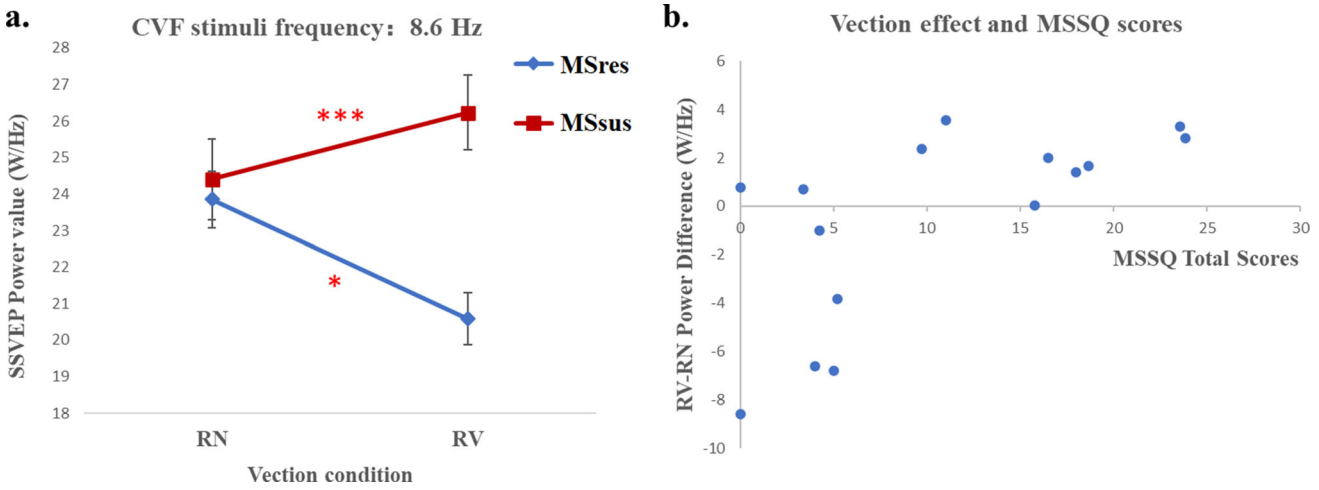

Fig. 3 The effect of vection and MS susceptibility on SSVEP power. *Note*: ***$p = 0.001$, *$p < 0.05$. **a** The interaction effect of vection and MS susceptibility on SSVEP power. Note that the illustration of interaction effect is plotted with the covariates (the general SSVEP power of RC condition) fixed at 25.4W/Hz for 8.6 Hz. **b** the scatter plot for SSVEP indicators of vection effect ($SSVEP_{RV} - SSVEP_{RN}$) and MS susceptibility

two MS groups. Results showed that: for MSres group, the SSVEP response significantly reduced during vection [$t(6) = 2.490$, $p = 0.047$, Cohen's $d = 0.941$]; for MSsus group, the SSVEP response significantly increased during vection [$t(7) = -5.311$, $p = 0.001$, Cohen's $d = 1.877$]. As for 12 Hz (PVF stimuli frequency), no significant effect was found for simple-main effects or simple-interaction effect.

MSSQ reports

We used the difference in SSVEP power between RV and RN ($VecEffect = SSVEP_{RV} - SSVEP_{RN}$) as the SSVEP indicators for vection effect. Correlation analysis showed that the SSVEP indicator of vection at 8.6 Hz ($VecEffec\ t_{8.6Hz}$) was positively correlated with MSSQ scores of participants (Pearson's $r = 0.658$, $p = 0.008$, see Fig. 3b for scatterplot), where individuals with higher MSSQ scores demonstrated stronger SSVEP responses during vection as compared to no-vection condition. This result supported the **H1b** (the vection effect size was correlated with individual MS susceptibility).

To further explore how the individual MSSQ scores can predict the vection effects, we then conducted a stepwise regression analysis using the two subscale scores (MSSQ_A & MSSQ_C) and total scores of MSSQ as predictors. Results showed that MSSQ_C (the recalled MS symptoms in the childhood of participants) had the best prediction power on the SSVEP indicators of vection (R^2=0.44, p = 0.007; see Table 3 for summary), excluding all other predictors from the model.

SSQ reports

Regression analysis revealed that the vection effects can predict the severity of MS symptoms of individual participants, which also supported the **H1b.** Stepwise regression analysis using the SSVEP indicators of vection effect ($VecEffec\ t_{8.6Hz}$ & $VecEffec\ t_{12Hz}$) as predictors were conducted for each subscale and the total scale of post-SSQ (see Table 3 for model and coefficients statistics). The coefficients of $VecEffec\ t_{8.6Hz}$ in the models for all post-SSQ scales were positive, suggesting that the higher was the increment of SSVEP power in CVF, the stronger was the MS symptoms. Moreover, the coefficients of $VecEffec\ t_{12Hz}$ was always negative, suggesting that the higher was the increment of SSVEP power in PVF, the lighter was the MS symptoms.

In general, the adjusted-R^2 across models suggested that the combination of two vection indicators showed best prediction power on post-SSQ scores, without any indicator excluded from the model, suggesting that CVF and PVF vection indicators might associate with different components in the generation of MS symptoms.

Note that when both MSSQ scores and SSVEP indicators of vection effect were added in the models to predict the MS symptoms, only SSVEP indicators of vection effect were kept by stepwise regression model and the MSSQ scores were excluded. Also, it is worth noting that the overall symptom of all participants was kept quite mild (the largest post-SSQ scores is 12.48 out of 40). The block exposure time was controlled to be short (192 s) with sufficient rest between blocks, to avoid the influence of severe MS symptoms on EEG responses. None of the

Table 3 Summary of regression models for vection effects and post-SSQ scores

Dependent	Predictors	Standardized Coefficients	R^2	Adjusted-R^2	F
VecEffec $t_{8.6Hz}$	MSSQ_C	0.666**	0.444	0.401	10.376**
		(p = 0.007)			(p = 0.007)
	MSSQ_A	Excluded			
Post-SSQ_T	*VecEffec* $t_{8.6Hz}$	0.599*	0.507	0.425	6.177*
		(p = 0.014)			(p = 0.014)
	VecEffec t_{12Hz}	− 0.545*			
		(p = 0.022)			
Post-SSQ_O	*VecEffec* $t_{8.6Hz}$	0.544*	0.562	0.489	7.695**
		(p = 0.017)			(p = 0.007)
	VecEffec t_{12Hz}	− 0.654**			
		(p = 0.006)			
Post-SSQ_D	*VecEffec* $t_{8.6Hz}$	0.582*	0.465	0.376	5.219*
		(p = 0.020)			(p = 0.023)
	VecEffec t_{12Hz}	− 0.512*			
		(p = 0.036)			
Post-SSQ_N	*VecEffec* $t_{8.6Hz}$	0.512	0.262	0.205	4.671
		(p = 0.051)			(p = 0.051)
	VecEffec t_{12Hz}	Excluded			

**$p < 0.01$, *$p < 0.05$. The vection effect size ($VecEffect = SSVEP_{RV} - SSVEP_{RN}$) are SSVEP indicators calculated by the SSVEP power at RV subtract the power at RN. *VecEffec* $t_{8.6Hz}$ and *VecEffec* t_{12Hz} represent the effect of SSVEP power at 8.6 Hz and 12 Hz respectively. For each dependent, only the model selected by the highest Adjusted-R^2 is reported. Post-SSQ_T, Post-SSQ_O, Post-SSQ_D, Post-SSQ_N represent the score of post-SSQ total scale, the ocular motor symptom subscale, the disorientation symptom subscale and the nausea symptom subscale respectively. Note that MSSQ scores have less prediction power than *VecEffect* on post-SSQ scores

participants reported obvious nausea, vomiting or other severe unpleasant feelings during the experiment.

Discussion

This study examined the SSVEP response to roll vection-inducing stimulation of people with different MS susceptibilities. We will elaborate on two major findings: (a) the differentiated SSVEP response to CVF and PVF visual stimulation for different MS sensitivity groups; (b) identified SSVEP changes as neural correlates for vection and MS susceptibility. Finally, potential applications and limitations are discussed.

Differentiated SSVEP response for different MS groups

As expected, we observed that the SSVEP power response to PVF (12 Hz) and CVF (8.6 Hz) stimulation frequencies exhibited different topographies. We found that the strongest response to PVF stimulation at 12 Hz was centered at the parietal-occipital region (Pz electrode, Fig. 2), with no topographical difference between the MS groups. For CVF stimulation, however, differential topographical responses were found between MSres and MSsus participants. The strongest SSVEP response for CVF stimulation of MSres participants was centered at the occipital region (Oz electrode). For the MSsus groups, the strongest SSVEP response was observed in the right-middle-occipital region (P4 electrode). The differentiated topography for SSVEP responses to CVF and PVF stimulations of MSres group was consistent with previous knowledge and retinotopic mapping studies (Bridge 2011). CVF checkerboard stimuli lead to strong activities in occipital regions (around the occipital pole and calcarine fissure) for contrast processing (Bach and Ullrich 1997; Di Russo et al. 2005; Griffis et al. 2016), while the rotating PVF stimulation led to stronger response in the parietal-occipital regions (Pitzalis et al. 2013; Uesaki and Ashida 2015; Wada et al. 2016) indicating PVF ambient information processing (e.g. large motion patterns).

Of interest are those MSsus participants showing a lateralization effect at P4 for CVF stimulation (Fig. 2a). It has been suggested that SSVEP responses distributed around P4 reflect activities in the right-middle-occipital region

(Bayram et al. 2011; Ji et al. 2019) and this region is known to be the vestibular region in right-handed participants (Dieterich et al. 2003). In this study, all participants are right-handed. Previous research also observed a right-hemisphere lateralization of alpha band SSVEP at the P4 electrode during vection. This lateralization effect has been interpreted as the coordination with sensory systems when sensory conflicts exist in self-motion perception (Dowsett et al. 2020). According to this, the lateralization in susceptible people might be because they experience stronger inconsistency between stationary CVF stimulation and self-motion perception. Another possible explanation is that MSsus people have impaired inter-hemispheric synchronization in parietal-temporal regions under vection-inducing stimulation (Miyazaki et al. 2015; Wei et al. 2019). This could then lead to an unbalanced response in right-hemisphere for susceptible people. Although the mechanism requires further investigation, the current finding presents clues in revealing the neural mechanism of sensory conflict. It is worth mentioning that this obvious topographical feature of susceptible people can also be developed into an objective indicator for screening MS susceptibility.

SSVEP power as indicators of vection and MS susceptibility

Participants showed different SSVEP correlates of vection depending on their MS susceptibility:

1. For SSVEP power at CVF frequency (8.6 Hz), the MSres group showed significant decreased responses during the vection period as compared to the no-vection period ($p = 0.047$, Cohen's $d = 0.941$), while the MSsus group demonstrated significant increased responses ($p = 0.001$, Cohen's $d = 1.877$, see Sect. "Vection state effects", Fig. 3a). Furthermore, participants with higher susceptibility to MS exhibited higher SSVEP responses (Fig. 3b, Pearson's $r = 0.658$, $p = 0.008$). These findings are consistent with previous behavioral studies which reported that the CVF task performance was impaired for MSsus participants and enhanced for MSsus participants (Wei et al. 2017a, 2018).

This interesting phenomenon agrees with sensory conflict theory (Reason 1978) and the 'reciprocal inhibition hypothesis' (Brandt et al. 1998, 2002) which suggested that the suppression of visual neurological response shall related to less sensory conflict and less MS. Several EEG studies (Stróżak et al. 2016; Thilo et al. 2003), which reported suppressed VEPs response at occipital electrodes during vection, were also consistent with our finding. Note that in Stróżak and Thilo's research, no evidence of MS was reported, as this is not the focus of their work. In the current study, we further revealed that (1) MS susceptibility questionnaire was correlated to the individual vection effect size measured by SSVEP; (2) moreover, this SSVEP correlates of vection can predict MS symptoms of individuals, with better prediction power than MSSQ scores (Table 3). Therefore, our findings complement current theory by revealing that the suppression of neurological visual response is closely associated with MS.

2. The significant interaction between frequency (CVF vs PVF stimulation) and vection accompanying the simple effect results supported our **H2** that the suppression of visual system is associated with CVF rather than PVF. Unlike the CVF frequency (8.6 Hz), for PVF frequency (12 Hz), we did not find any vection suppression effects. Furthermore, we observed that vection effects of PVF can predict MS symptoms in the opposite direction to the CVF responses, which is consistent with previous finding that enhanced vection responses at PVF was correlated with better resistance to MS (Wei et al. 2018). This result further supported that the processing of PVF and CVF stimuli played different roles in the generation of MS.

In summary, MSres people demonstrate reduced SSVEP responses under vection, while MSsus people showed opposite effects. Moreover, the power changes of SSVEP showed good potential as indicators for MS susceptibility. The feature of SSVEP power (Sect. "SSVEP power as indicators of vection and MS susceptibility") and topography (Sect. "Differentiated SSVEP response for different MS groups") not only contribute objective neural evidence associated with MS susceptibility, they can be incorporated in future objective indicators for screening MS susceptibility, which would be desirable both for academic research and industry (Guo et al. 2017; IWA 3 2005).

Potential applications

This study supports that suppressed visual activities in CVF were correlated with better resistance to MS and fewer MS symptoms. This might provide theoretical support for future research on VR designs or visual training to better prevent MS. Moreover, the SSVEP correlates revealed in this study can predict following MS symptoms reported by participants, it is possible that with further validations, the SSVEP power and topographies identified in current study can be developed into new objective measures for MS susceptibility, which is beneficial for the industry applications (Guo et al. 2017; IWA 3 2005).

Potential limitations and validations

As the frequencies and the visual stimuli types selected for CVF and PVF stimulations were not the same, there might be confounding factor when CVF and PVF response were compared directly. For example, different stimulation frequencies may exhibit different baseline powers and lead to different effect sizes under vection-inducing stimulation. However, since we have added the general response of SSVEP power at each frequency as correlates in the model, and this study was mainly focus on the vection effects which were compared within each frequency (each type of visual stimulation), this issue was unlikely to influence the findings we reported.

To validate the statistical power of current study, we conducted a post-hoc power analysis using the G*Power software (Faul et al. 2007) to obtain the power $(1-\beta)$ of the tests supporting our hypotheses. Regarding H1, the results were mainly supported by the significant simple-interaction effect of vection × MS group [$F(1,11) = 11.911$, $p = 0.005$, Cohen's $f = 0.916$]. Regarding H2, the results were mainly supported by the significant simple-interaction effect vection × frequency × MS susceptibility [$F(1,11) = 11.886$, $p = 0.005$, Cohen's $f = 0.915$]. When alpha equals 0.05, effect size (Cohen's f) equals 0.915 (or 0.916), and the sample size (N) equals 7/8 for two groups, the achieved power $(1-\beta)$ calculated for within-between interaction effect is 0.999. Nevertheless, we acknowledge that current results were based on a limited sample of university students, and further validation with a larger sample in a wider population is desirable.

Conclusion

This study identified alpha band SSVEP correlates for vection perception and MS susceptibility. In summary, the finding supports the sensory conflict theory and reciprocal inhibition hypothesis (Brandt et al. 1998). To the best of our knowledge, this is the first study that has reported SSVEP signatures for MS susceptibility. As SSVEP possess higher noise resistance than common VEPs, given further validation, the identified SSVEP signatures could contribute to better objective measures for MS susceptibility in the future.

Supplementary Information The online version contains supplementary material available at https://doi.org/10.1007/s11571-023-09991-7.

Acknowledgements The authors would like to thank the Science, Technology, and Innovation Commission of Shenzhen Municipality for partially supporting the work under Project No. JCYJ20170413173515472. This study was also partially funded by the Hong Kong Research Grants Council under Project No. 16200915 and National Natural Science Foundation of China under Project No. 32200923.

Data availability The data and code generated and analyzed during the current study are not publicly available for legal/ethical reasons but are available from the corresponding author on reasonable request.

References

Bach M, Ullrich D (1997) Contrast dependency of motion-onset and pattern-reversal VEPs: interaction of stimulus type, recording site and response component. Vis Res 37(13):1845–1849. https://doi.org/10.1016/S0042-6989(96)00317-3

Barry RJ, Palmisano S, Schira MM, De Blasio FM, Karamacoska D, MacDonald B (2014) EEG markers of visually experienced self-motion (vection). Front Hum Neurosci. https://doi.org/10.3389/conf.fnhum.2014.216.00013

Bayram A, Bayraktaroglu Z, Karahan E, Erdogan B, Bilgic B, Özker M, Kasikci I, Duru AD, Ademoglu A, Öztürk C, Arikan K, Tarhan N, Demiralp T (2011) Simultaneous EEG/fMRI analysis of the resonance phenomena in steady-state visual evoked responses. Clin EEG Neurosci 42(2):98–106. https://doi.org/10.1177/155005941104200210

Berti S, Keshavarz B (2020) Neuropsychological approaches to visually-induced vection: an overview and evaluation of neuroimaging and neurophysiological studies. Multisens Res 34(2):153–186. https://doi.org/10.1163/22134808-BJA10035

Berti S, Haycock B, Adler J, Keshavarz B (2018) Early cortical processing of vection-inducing visual stimulation as measured by event-related brain potentials (ERP). Displays. https://doi.org/10.1016/j.displa.2018.10.002

Brainard DH (1997) The psychophysics toolbox. Spat vis 10(4):433–436. https://doi.org/10.1163/156856897X00357

Brandt T, Bartenstein P, Janek A, Dieterich M (1998) Reciprocal inhibitory visual–vestibular interaction. Visual motion stimulation deactivates the parieto-insular vestibular cortex. Brain 121(9):1749–1758

Brandt T, Glasauer S, Stephan T, Bense S, Yousry TA, Deutschlander A, Dieterich M (2002) Visual-vestibular and visuovisual cortical interaction: new insights from fMRI and pet. Ann N Y Acad Sci 956:230–241

Bridge H (2011) Mapping the visual brain: how and why. Eye (london) 25(3):291–296. https://doi.org/10.1038/eye.2010.166

Camfield DA, Scholey A, Pipingas A, Silberstein R, Kras M, Nolidin K, Wesnes K, Pase M, Stough C (2012) Steady state visually evoked potential (SSVEP) topography changes associated with cocoa flavanol consumption. Physiol Behav 105(4):948–957. https://doi.org/10.1016/j.physbeh.2011.11.013

Delorme A, Makeig S (2004) EEGLAB: An open source toolbox for analysis of single-trial EEG dynamics including independent component analysis. J Neurosci Methods 134(1):9–21. https://doi.org/10.1016/j.jneumeth.2003.10.009

Di Russo F, Pitzalis S, Spitoni G, Aprile T, Patria F, Spinelli D, Hillyard SA (2005) Identification of the neural sources of the pattern-reversal VEP. Neuroimage 24(3):874–886. https://doi.org/10.1016/j.neuroimage.2004.09.029

Dieterich M, Bense S, Lutz S, Drzezga A, Stephan T, Bartenstein P, Brandt T (2003) Dominance for vestibular cortical function in the non-dominant hemisphere. Cereb Cortex 13(9):994–1007. https://doi.org/10.1093/CERCOR/13.9.994

Dowsett J, Herrmann CS, Dieterich M, Taylor PCJ (2020) Shift in lateralization during illusory self-motion: EEG responses to

visual flicker at 10 Hz and frequency-specific modulation by tACS. Eur J Neurosci 51(7):1657–1675. https://doi.org/10.1111/EJN.14543

Farmer AD, Ban VF, Coen SJ, Sanger GJ, Barker GJ, Gresty MA, Giampietro VP, Williams SC, Webb DL, Hellström PM, Andrews PLR, Aziz Q (2015) Visually induced nausea causes characteristic changes in cerebral, autonomic and endocrine function in humans. J Physiol 593(5):1183–1196. https://doi.org/10.1113/jphysiol.2014.284240

Faul F, Erdfelder E, Lang AG, Buchner A (2007) G*Power 3: a flexible statistical power analysis program for the social, behavioral, and biomedical sciences. Behav Res Methods 39(2):175–191. https://doi.org/10.3758/BF03193146/METRICS

Golding JF (1998) Motion sickness susceptibility questionnaire revised and its relationship to other forms of sickness. Brain Res Bull 47(5):507–516

Golding JF (2006) Motion sickness susceptibility. Auton Neurosci 129(1–2):67–76. https://doi.org/10.1016/j.autneu.2006.07.019

Golding JF, Doolan K, Acharya A, Tribak M, Gresty MA (2012) Cognitive cues and visually induced motion sickness. Aviat Space Environ Med 83(5):477–482. https://doi.org/10.3357/ASEM.3095.2012

Griffin MJ (1990) Handbook of human vibration. Academic Press, New York

Griffis J, Elkhetali A, Burge W, Chen R, Bowman A, Szaflarski J, Visscher K (2016) Retinotopic patterns of functional connectivity between V1 and large-scale brain networks during resting fixation. Unpublished Results, 1. https://doi.org/10.1017/CBO9781107415324.004

Guo CCT, Chen DJZ, Wei IY, So RHY, Cheung RTF (2017) Correlations between individual susceptibility to visually induced motion sickness and decaying time constant of after-nystagmus. Appl Ergon 63:1–8. https://doi.org/10.1016/j.apergo.2017.03.011

IWA 3 (2005) International Workshop Agreement 3: Image safety—reducing the incidence of undesirable biomedical effects caused by visual image sequences (IWA 3:2005). International Organisation of Standardisation

Ji H, Chen B, Petro NM, Yuan Z, Zheng N, Keil A (2019) Functional source separation for EEG-fMRI fusion: application to steady-state visual evoked potentials. Front Neurorobot 13:24. https://doi.org/10.3389/FNBOT.2019.00024/BIBTEX

Kayser J, Tenke CE (2006a) Principal components analysis of Laplacian waveforms as a generic method for identifying ERP generator patterns: I. Evaluation with auditory oddball tasks. Clin Neurophysiol 117(2):348–368. https://doi.org/10.1016/j.clinph.2005.08.034

Kayser J, Tenke CE (2006b) Principal components analysis of Laplacian waveforms as a generic method for identifying ERP generator patterns: II. Adequacy of low-density estimates. Clin Neurophysiol 117(2):369–380. https://doi.org/10.1016/j.clinph.2005.08.033

Kennedy RS, Lane NE, Berbaum KS, Lilienthal MG (1993) Simulator Sickness Questionnaire: an enhanced method for quantifying simulator sickness. Int J Aviat Psychol 3(3):203–220. https://doi.org/10.1207/s15327108ijap0303_3

Keshavarz B, Berti S (2014) Integration of sensory information precedes the sensation of vection: a combined behavioral and event-related brain potential (ERP) study. Behav Brain Res 259:131–136. https://doi.org/10.1016/j.bbr.2013.10.045

Keshavarz B, Campos JL, Berti S (2015a) Vection lies in the brain of the beholder: EEG parameters as an objective measurement of vection. Front Psychol. https://doi.org/10.3389/fpsyg.2015.01581

Keshavarz B, Riecke BE, Hettinger LJ, Campos JL (2015b) Vection and visually induced motion sickness: how are they related? Front Psychol 6:472. https://doi.org/10.3389/fpsyg.2015.00472

Keshavarz B, Hecht H, Lawson B (2014) Visually induced motion sickness: causes, characteristics, and countermeasures, pp 647–698. https://doi.org/10.1201/b17360-32

Kleinschmidt A, Thilo KV, Büchel C, Gresty MA, Bronstein AM, Frackowiak RSJ (2002) Neural correlates of visual-motion perception as object- or self-motion. Neuroimage 16(4):873–882

Klimesch W (2012) Alpha band oscillations, attention, and controlled access to stored information. Trends Cogn Sci 16(12):606–617. https://doi.org/10.1016/J.TICS.2012.10.007

Lopez-Calderon J, Luck SJ (2014) ERPLAB: an open-source toolbox for the analysis of event-related potentials. Front Hum Neurosci 8(April):213. https://doi.org/10.3389/fnhum.2014.00213

Luck SJ (2005) An introduction to the event-related potential technique. https://books.google.com.hk/books/about/An_Introduction_to_the_Event_related_Pot.html?id=r-BqAAAAMAAJ&pgis=1

Miyazaki J, Yamamoto H, Ichimura Y, Yamashiro H, Murase T, Yamamoto T, Umeda M, Higuchi T (2015) Inter-hemispheric desynchronization of the human MT+ during visually induced motion sickness. Exp Brain Res. https://doi.org/10.1007/s00221-015-4312-y

Mognon A, Jovicich J, Bruzzone L, Buiatti M (2011) ADJUST: an automatic EEG artifact detector based on the joint use of spatial and temporal features. Psychophysiology 48(2):229–240. https://doi.org/10.1111/j.1469-8986.2010.01061.x

Morgan ST, Hansen JC, Hillyard SA (1996) Selective attention to stimulus location modulates the steady-state visual evoked potential. Proc Natl Acad Sci USA 93(10):4770–4774. https://doi.org/10.1073/pnas.93.10.4770

Müller MM, Picton TW, Valdes-Sosa P, Riera J, Teder-Sälejärvi WA, Hillyard SA (1998) Effects of spatial selective attention on the steady-state visual evoked potential in the 20–28 Hz range. Cogn Brain Res 6(4):249–261. https://doi.org/10.1016/S0926-6410(97)00036-0

Napadow V, Sheehan JD, Kim J, Lacount LT, Park K, Kaptchuk TJ, Rosen BR, Kuo B (2013) The brain circuitry underlying the temporal evolution of nausea in humans. Cereb Cortex 23(4):806–813. https://doi.org/10.1093/cercor/bhs073

Niedermeyer E, Lopes da Silva FH (2005) Electroencephalography: basic principles, clinical applications, and related fields. Lippincott Williams & Wilkins, Philadelphia

Oostenveld R, Fries P, Maris E, Schoffelen JM (2011) FieldTrip: open source software for advanced analysis of MEG, EEG, and invasive electrophysiological data. Comput Intell Neurosci 2011:1–9. https://doi.org/10.1155/2011/156869

Palmisano S, Allison RS, Schira MM, Barry RJ (2015) Future challenges for vection research: definitions, functional significance, measures, and neural bases. Front Psychol 6:193. https://doi.org/10.3389/fpsyg.2015.00193

Pelli DG (1997) The VideoToolbox software for visual psychophysics: transforming numbers into movies. Spat vis 10(4):437–442. https://doi.org/10.1163/156856897X00366

Pitzalis S, Bozzacchi C, Bultrini A, Fattori P, Galletti C, Di Russo F (2013) Parallel motion signals to the medial and lateral motion areas V6 and MT+. Neuroimage 67:89–100. https://doi.org/10.1016/j.neuroimage.2012.11.022

Reason JT (1978) Motion sickness adaptation: a neural mismatch model. J R Soc Med 71(11):819–829

Riecke BE (2011) Virtual reality (J-J Kim, ed). InTech. https://doi.org/10.5772/553

Riecke BE, Schulte-Pelkum J, Avraamides MN, Bülthoff, HH (2004, October) Enhancing the visually induced selfmotion illusion (vection) under natural viewing conditions in virtual reality. In

7th Annual International Workshop Presence (PRESENCE 2004) (pp. 125–132). UPV. https://hdl.handle.net/11858/00-001M-0000-0013-D7A1

Stróżak P, Francuz P, Augustynowicz P, Ratomska M, Fudali-Czyż A, Bałaj B (2016) ERPs in an oddball task under vection-inducing visual stimulation. Exp Brain Res 1:10. https://doi.org/10.1007/s00221-016-4748-8

Thilo KV, Kleinschmidt A, Gresty MA (2003) Perception of self-motion from peripheral optokinetic stimulation suppresses visual evoked responses to central stimuli. J Neurophysiol 90(2):723–730. https://doi.org/10.1152/jn.00880.2002

Uesaki M, Ashida H (2015) Optic-flow selective cortical sensory regions associated with self-reported states of vection. Front Psychol 6:775. https://doi.org/10.3389/fpsyg.2015.00775

Vialatte FB, Maurice M, Dauwels J, Cichocki A (2010) Steady-state visually evoked potentials: focus on essential paradigms and future perspectives. In: Progress in neurobiology, vol 90, issue 4, pp 418–438. https://doi.org/10.1016/j.pneurobio.2009.11.005

Vilhelmsen K, van der Weel FR, van der Meer ALH (2015) A high-density EEG study of differences between three high speeds of simulated forward motion from optic flow in adult participants. Front Syst Neurosci. https://doi.org/10.3389/fnsys.2015.00146

Wada A, Sakano Y, Ando H (2016) Differential responses to a visual self-motion signal in human medial cortical regions revealed by wide-view stimulation. Front Psychol 7:309. https://doi.org/10.3389/fpsyg.2016.00309

Warren WH, Kurtz KJ (1992) The role of central and peripheral vision in perceiving the direction of self-motion. Percept Psychophys 51(5):443–454. https://doi.org/10.3758/BF03211640

Webb NA, Griffin MJ (2003) Eye movement, vection, and motion sickness with foveal and peripheral vision. Aviat Space Environ Med 74(6 Pt 1):622–625

Wei Y, Fu X, So RHY (2017a) Does your attention allocation affect how motion sick you can get. Contemp Ergonom 2017:167–174

Wei Y, Zheng J, So R (2017b) Duration of vection generated by rotating dot patterns in peripheral correlates with VEP suppression in central visual field. J vis 17(10):597. https://doi.org/10.1167/17.10.597

Wei Y, Zheng J, So RHY (2018) Allocating less attention to central vision during vection is correlated with less motion sickness. Ergonomics 61(7):933–946. https://doi.org/10.1080/00140139.2018.1427805

Wei Y, Okazaki YO, So RHY, Chu WCW, Kitajo K (2019) Motion sickness-susceptible participants exposed to coherent rotating dot patterns show excessive N2 amplitudes and impaired theta-band phase synchronization. Neuroimage 202:116028. https://doi.org/10.1016/j.neuroimage.2019.116028

Yang JX, Guo CT, So RHY, Cheung RTF (2011) Effects of eye fixation on visually induced motion sickness: are they caused by changes in retinal slip velocity? https://doi.org/10.1177/1071181311551254

Zhang L-L, Wang J-Q, Qi R-R, Pan L-L, Li M, Cai Y-L (2015) Motion sickness: current knowledge and recent advance. CNS Neurosci Ther. https://doi.org/10.1111/cns.12468

Zhao Y (2017) Identifying vestibular and visual cortical response during circular vection among people with different susceptibility to motion sickness [The Hong Kong University of Science and Technology]. https://doi.org/10.14711/thesis-b1781036